

## Community dynamics and activity of *nirS*-harboring denitrifiers in sediments of the Indus River Estuary

Fozia<sup>a</sup>, Yanling Zheng<sup>a,b,c,\*</sup>, Lijun Hou<sup>a,\*\*</sup>, Zongxiao Zhang<sup>a</sup>, Dengzhou Gao<sup>b,c</sup>, Guoyu Yin<sup>b,c</sup>, Ping Han<sup>a,b,c</sup>, Hongpo Dong<sup>a</sup>, Xia Liang<sup>a</sup>, Yi Yang<sup>b,c</sup>, Min Liu<sup>b,c</sup>

<sup>a</sup> State Key Laboratory of Estuarine and Coastal Research, East China Normal University, 500 Dongchuan Road, Minhang District, Shanghai 200241, China

<sup>b</sup> School of Geographic Sciences, East China Normal University, 500 Dongchuan Road, Minhang District, Shanghai 200241, China

<sup>c</sup> Key Laboratory of Geographic Information Science (Ministry of Education), East China Normal University, 500 Dongchuan Road, Minhang District, Shanghai 200241, China

### ARTICLE INFO

#### Keywords:

Denitrification

Nitrogen

*nirS* gene

The Indus River Estuary

### ABSTRACT

Denitrification is an important pathway for reactive nitrogen removal from aquatic ecosystems. In this study, the biodiversity, abundance, and activity of cytochrome *cd*<sub>1</sub>-type nitrate reductase gene (*nirS*)-harboring denitrifiers in the sediments of the Indus River Estuary were examined by molecular and isotope-tracing techniques. Results showed that the *nirS*-harboring denitrifier communities showed significant geographical variations along the estuarine salinity gradient. Real-time quantitative PCR showed that the abundance of *nirS*-harboring denitrifiers ranged from  $5.3 \times 10^6$  to  $2.5 \times 10^8$  copies  $g^{-1}$ , without significant spatiotemporal variation. The potential rates of denitrification varied from 0.01 to 6.27  $\mu\text{mol N kg}^{-1} \text{h}^{-1}$  and correlated significantly to TOC and Fe(II) ( $P < 0.05$ ). On the basis of <sup>15</sup>N isotope-tracing experiments, the denitrification process contributed 18.4–99.4% to the total nitrogen loss in the sediments of the Indus River Estuary. This study provides novel insights into the microbial mechanism of nitrogen removal process in estuarine ecosystems.

### 1. Introduction

Nitrogen (N) is an essential constituent of living organisms, but excess amount of nitrogen can be harmful to aquatic ecosystems (Fowler et al., 2013; Galloway, 2013; Gruber and Galloway, 2008; Luo et al., 2018). In recent decades, reactive nitrogen loading in most aquatic environments has greatly increased, because of human activities such as the discharge of industrial and municipal wastes, fertilizer application, and fossil fuel combustion (Booth and Campbell, 2007; Galloway et al., 2008, 2004; Vitousek and Howarth, 1991). The accumulation of reactive nitrogen in aquatic ecosystems has caused severe eutrophication, harmful algal blooms, hypoxia, anoxia, loss of biodiversity and seawater acidification (Booth and Campbell, 2007; Deegan et al., 2012; Diaz and Rosenberg, 2008; Galloway et al., 2004; Glibert et al., 2005; Paerl, 1997). In this context, a better understanding of nitrogen removal and associated microbial mechanisms is crucial for controlling the pollution of reactive nitrogen and improving water quality in aquatic ecosystems.

Denitrification is a known and sophisticated process eliminating

reactive nitrogen from aquatic ecosystems (Dalsgaard et al., 2012; Zumft, 1997). It is a primary contributor to the removal of reactive nitrogen in natural ecosystems, compared with anaerobic oxidation of ammonium (anammox) (Dalsgaard et al., 2012). Under an anaerobic condition, denitrifiers respire nitrate ( $\text{NO}_3^-$ ) to nitrite ( $\text{NO}_2^-$ ), nitric oxide (NO), nitrous oxide ( $\text{N}_2\text{O}$ ), and at last to  $\text{N}_2$  (Santoro et al., 2011; Zumft, 1997). Denitrification is a biological process for fixed N removal from aquatic and terrestrial ecosystems, which is restricted by different groups of microorganisms (Zumft, 1997). These diverse phylogenetic groups of microorganisms are responsible for the denitrification process by using various types of enzymes, such as nitrate reductase (Nar), nitrite reductase (Nir), nitric oxide reductase (Nor), and nitrous oxide reductase (Nos) (Zumft, 1997). In denitrification,  $\text{NO}_2^-$  reduction to NO is catalyzed either by cytochrome *cd*<sub>1</sub>-*nirS*  $\text{NO}_2^-$  reductase or copper containing *nirK*  $\text{NO}_2^-$  reductase (Coyne et al., 1989; Hochstein and Tomlinson, 2003; Sakurai and Kataoka, 2007; Zumft, 1997). Although these two genes are similar in physiological and functional manner, but possess different skeleton (Glockner et al., 1993; Zumft, 1997). The *nirS* gene is generally used as a gene marker for the

\* Correspondence to: Y. Zheng, State Key Laboratory of Estuarine and Coastal Research, East China Normal University, 500 Dongchuan Road, Minhang District, Shanghai 200241, China.

\*\* Corresponding author.

E-mail addresses: [ylzheng@geo.ecnu.edu.cn](mailto:ylzheng@geo.ecnu.edu.cn) (Y. Zheng), [ljhou@sklec.ecnu.edu.cn](mailto:ljhou@sklec.ecnu.edu.cn) (L. Hou).

<https://doi.org/10.1016/j.marpolbul.2020.110971>

Received 26 November 2019; Received in revised form 4 February 2020; Accepted 10 February 2020

Available online 15 February 2020

0025-326X/ © 2020 Elsevier Ltd. All rights reserved.

identification of denitrifying bacteria in aquatic ecosystems (Coyne et al., 1989; Glockner et al., 1993; Zumft, 1997). The association between denitrification and functional microbial dynamics remains largely uncertain for a specific aquatic ecosystem.

In the present work, the Indus River Estuary was selected as a representative study region to determine the biodiversity, abundance, and contribution of *nirS*-harboring denitrifiers in the nitrogen removal process. The Indus River originates in Tibet Plateau near Lake Manasarovar, with a total length of 3200 km approximately, a drainage basin area of  $9.7 \times 10^5 \text{ km}^2$ , a deltaic area of  $3 \times 10^4 \text{ km}^2$ , and annual sediment discharge of  $2 \times 10^{11} \text{ kg}$  (Ali and de Boer, 2008; Davidson, 2016; Hussain, 2011). The annual rainfall is low (about 180–220 mm), resulting in the sub-tropical and arid environmental condition (Inam et al., 2008; Kidwai et al., 2019). The tide in the Indus River Estuary is semidiurnal, with an amplitude of about 2.7 m (Saifullah et al., 2002). Nowadays,  $> 3 \times 10^6 \text{ t}$  of nitrogen is annually entered into the Indus River basin due to human activities such as excessive fertilizer use in agriculture and improper disposal of wastewater (Amin et al., 2017; Wang et al., 2019), which has caused serious environmental problems such as eutrophication, hypoxia, and harmful algal blooms in the Indus River Estuary (Kidwai et al., 2019; Kravtsova et al., 2009). Hence, the microbial reactive nitrogen loss is a primary concern in the Indus River Estuary. The aims of the present study were (a) to explore the biodiversity, abundance, and distribution pattern of *nirS*-harboring denitrifiers across the salinity gradient of the Indus River Estuary, (b) to elucidate the potential role of denitrifiers in the surface sediment of the Indus River Estuary, and (c) to investigate the potential links between the dynamics of *nirS*-harboring denitrifiers and environmental factors in the sediments of the Indus River Estuary. To the best of our knowledge, this is the first study to investigate the dynamics and potential role of *nirS*-harboring denitrifiers in the sediments of the Indus River Estuary.

## 2. Materials and methods

### 2.1. Sample collection

The Indus River Estuary, Pakistan, was selected as our sampling area. In the present study, a total of 12 sites were selected along the Indus River Estuary, including Thatta bridge (TB), Goth qaisrani (GQ), Babra road (BR), Allah rakhio (AR), Udero shrine (US), Jangi sar (JS), Dando (DD), Sajanjari (SW), Kharochan (KC), Main kharochan (MK), Keti bunder (KB) and Jamia masjid keti bunder (JK) (Fig. 1). A significant salinity gradient (0–36 ppt) was observed along the estuary of the Indus River. On the basis of the salinity difference, the sampling sites along the estuary were divided into 3 groups: freshwater sites (0 ppt, TB to US in winter and TB to MK in summer), low-salinity sites (1–15 ppt, JS to DD in winter), and high-salinity sites (16–36 ppt, SW to JK in winter and KB to JK in summer). At each sampling region, sediment samples (0–5 cm) were collected in triplicate in February (winter) and August (summer) 2017, respectively, with scaled stainless steel shovels. The shovels were cleaned and sterilized before sampling to avoid contamination. The collected sediment samples were stored in sterile polyethylene bags and sealed immediately. During the field surveys, near-bottom water (approximately 0.5 m above the surface sediment) samples were also collected with sterile polyethylene bottles for the measurement of denitrification rates. All the collected samples were transferred to laboratory on ice within 12 h. The sediment samples were homogenized as a composite mixture of each sampling site under helium condition and separated into two fractions after returned to the laboratory. One fraction was preserved at  $-80 \text{ }^\circ\text{C}$  for molecular microbial analyses, and the second fraction was preserved at  $4 \text{ }^\circ\text{C}$  for measurement of sediment physicochemical properties and denitrification rates.

### 2.2. Analyses of environmental characteristics

The water temperature, salinity, and pH were measured in situ by portable salt meter (CT-3086) and Mettler-Toledo pH meter. Sediment moisture content was calculated through the weight loss of a known amount of fresh sediment which was dried to a constant value at  $80 \text{ }^\circ\text{C}$  (Zheng et al., 2016). The extraction of sediment inorganic nitrogen was proceeded using 2 M KCl. Subsequently, the concentrations of ammonium ( $\text{NH}_4^+$ ),  $\text{NO}_3^-$ , and  $\text{NO}_2^-$  were measured by continuous-flow injection analysis (Skalar Analytical SAN+, Netherlands). The detection limit is  $0.5 \text{ } \mu\text{M}$  for ammonium ( $\text{NH}_4^+$ ) and  $0.1 \text{ } \mu\text{M}$  for  $\text{NO}_3^-$  and  $\text{NO}_2^-$  ( $\text{NO}_x^-$ ) (Hu et al., 2017). Sediment total organic carbon (TOC) was measured after acidification with 1 M HCl via Vario EL CN Elemental Analyzer (Elementar, Germany) (Zhang et al., 2015). Sediment sulfide was analyzed via methylene blue spectrophotometric method (Cline, 1969). The concentration of Fe(II) and Fe(III) was measured followed by our previous work (Zheng et al., 2019) and the references therein (Rodén and Lovley, 1993). Grain size of the sediment samples were measured on a LS 13 320 Laser grain sizer (Wang et al., 2016). All physicochemical characteristics were measured in triplicate (Table 1).

### 2.3. Measurement of denitrification rates

Denitrification rates were measured using the sediment-slurry methods combined with  $^{15}\text{N}$  isotope-tracing technique (Hou et al., 2013). Briefly, slurries were made from fresh sediment samples and helium-purged overlying water from each site at a volume ratio of 1:7 (sediment/water). Then, the resulting sediment slurries were transferred into a sequence of vials (12 mL, Exetainer, Labco) under a helium atmosphere, sealed with butyl rubber cork, and tightly capped. To remove residual  $\text{NO}_3^-$ ,  $\text{NO}_2^-$ , and  $\text{O}_2$ , these vials were pre-incubated for 24 h under approximate in situ temperature. After that, the vials were spiked with stock solutions of  $^{15}\text{NO}_3^-$  ( $^{15}\text{N}$  at 99%), and the resulting concentrations of  $^{15}\text{N}$  was about  $100 \text{ } \mu\text{M}$  in each vial. These vials were on average separated into two parts: the first group named as initial samples was inhibited by 200  $\mu\text{L}$  of 50%  $\text{ZnCl}_2$  as a microbial inhibitor and the second group named as terminal samples was inhibited by 50%  $\text{ZnCl}_2$  (200  $\mu\text{L}$ ) after 8 h of incubation.  $^{29}\text{N}_2$  and  $^{30}\text{N}_2$  concentrations during the incubations amended with  $^{15}\text{NO}_3^-$  were measured by membrane inlet mass spectrometry (MIMS) (HPR-40, Hiden Analytical, UK), with a detection limit of  $0.1 \text{ } \mu\text{mol N}_2 \text{ L}^{-1}$  (An and Gardner, 2002). The potential rates of denitrification and its contribution to total  $\text{N}_2$  production were calculated by the equations as described by Thamdrup and Dalsgaard (2002) and Trimmer et al. (2003). In brief, the production of  $^{29}\text{N}_2$  resulting from denitrification and anammox during the incubation were described in Eq. (1)

$$P_{29} = A_{29} + D_{29} \quad (1)$$

where  $P_{29}$  denotes the total production rates of  $^{29}\text{N}_2$ , and the production rates of  $^{29}\text{N}_2$  from denitrification and anammox were denoted as  $D_{29}$  and  $A_{29}$ , respectively.  $D_{29}$  was expressed by Eq. (2)

$$D_{29} = P_{30} \times 2 \times (1 - F_N) \times F_N^{-1} \quad (2)$$

where  $P_{30}$  denotes the total production rates of  $^{30}\text{N}_2$ ,  $F_N$  (%) denotes the  $^{15}\text{N}$  fraction in  $\text{NO}_3^-$  in the incubation slurries. The potential denitrification and anammox rates were calculated by Eqs. (3) and (4), respectively.

$$D_t = D_{29} + 2P_{30} \quad (3)$$

where  $D_t$  denotes the rates of denitrification.

$$A_{29} = P_{29} - D_{29} \quad (4)$$

where  $A_{29}$  denotes the rates of anammox. The contribution of

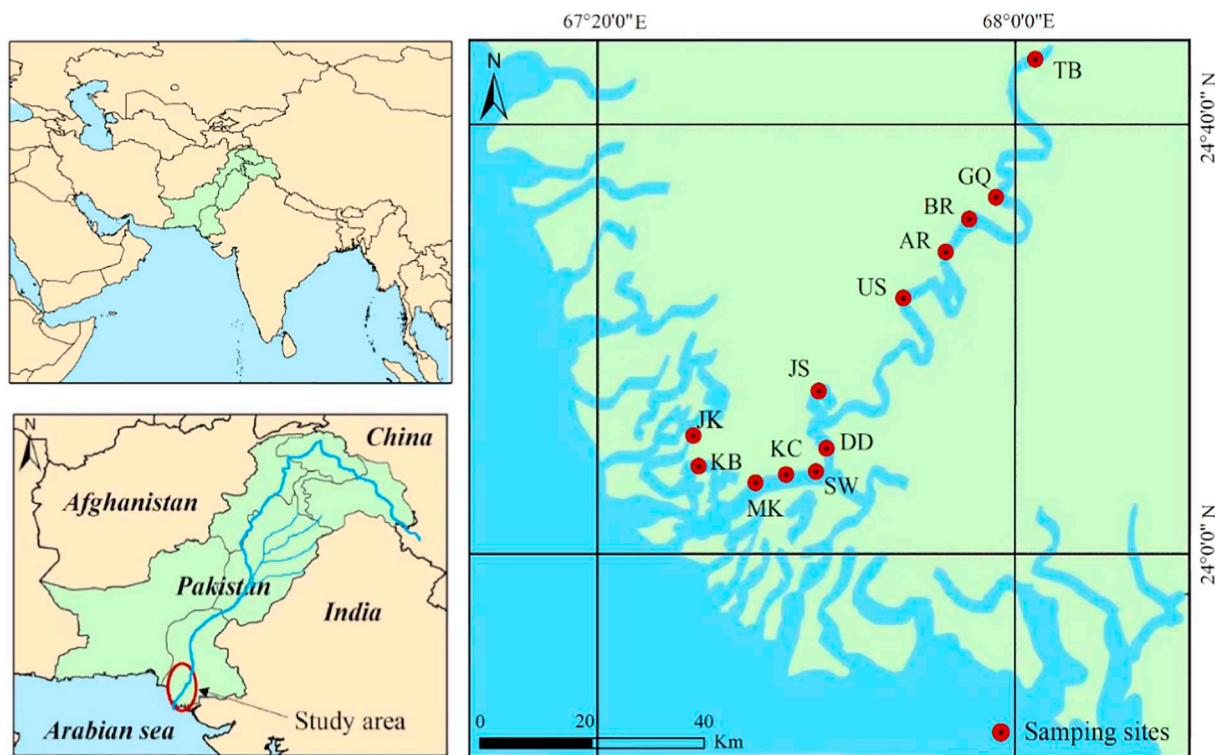


Fig. 1. Location of sampling sites of the Indus River Estuary, Pakistan.

**Table 1**  
Physicochemical characteristics of the samples in the Indus River Estuary.

Seasons	Sites	Salinity (‰) <sup>a</sup>	pH <sup>a</sup>	Temp (°C) <sup>a</sup>	M.S. (µm) <sup>b</sup>	M.C. (%) <sup>b</sup>	TOC (mg g <sup>-1</sup> ) <sup>b</sup>	Fe(II) (mg g <sup>-1</sup> ) <sup>b</sup>	Fe(III) (mg g <sup>-1</sup> ) <sup>b</sup>	NO <sub>3</sub> <sup>-</sup> (mg kg <sup>-1</sup> ) <sup>b</sup>	NO <sub>2</sub> <sup>-</sup> (mg kg <sup>-1</sup> ) <sup>b</sup>	NH <sub>4</sub> <sup>+</sup> (mg kg <sup>-1</sup> ) <sup>b</sup>	Sulfide (mg kg <sup>-1</sup> ) <sup>b</sup>
Winter	TB	0	8.4	16.1	123.0	25.0	5.6	0.019	0.021	6.5	0.05	196.8	1.7
	GQ	0	8.2	18.8	11.5	26.3	5.5	0.025	0.019	39.7	0.29	31.8	2.1
	BR	0	8.4	18.9	17.6	30.4	6.6	0.016	0.011	38.4	0.28	26.0	1.1
	AR	0	8.5	21.0	105.4	22.7	5.6	0.022	0.010	33.6	0.08	39.2	1.1
	US	0	8.3	20.0	16.3	23.8	4.6	0.021	0.013	11.5	0.17	21.8	0.7
	JS	11	8.4	19.7	15.3	28.9	8.8	0.014	0.031	30.8	0.19	24.2	1.5
	DD	12	8.5	21.0	11.2	26.9	7.0	0.016	0.022	17.1	0.13	10.3	1.6
	SW	23	8.4	20.0	21.4	26.0	5.4	0.015	0.024	18.5	0.52	32.2	0.0
	KC	25	7.5	21.5	16.3	32.2	5.3	0.016	0.016	21.4	0.19	237.4	0.1
	MK	26	8.4	21.6	11.6	34.1	7.7	0.002	0.035	52.8	0.43	257.3	0.4
	KB	36	8.4	21.0	10.7	33.8	6.0	0.016	0.024	34.0	0.19	177.2	0.1
	JK	33	8.4	26.0	11.1	30.1	8.6	0.016	0.026	16.7	0.12	79.2	0.3
	Summer	TB	0	8.5	27.9	29.9	20.2	1.9	0.005	0.003	16.6	0.30	24.4
GQ		0	8.1	28.0	13.3	29.7	5.9	0.011	0.020	52.7	0.76	62.8	1.2
BR		0	8.0	29.4	10.8	27.1	4.5	0.011	0.016	19.5	0.28	44.5	0.1
AR		0	8.1	29.0	35.8	22.0	3.1	0.008	0.018	9.4	0.08	43.4	0.0
US		0	8.1	30.0	47.6	23.9	5.4	0.015	0.020	19.5	0.12	74.1	0.0
JS		0	7.9	29.4	17.6	26.9	6.4	0.034	0.010	11.7	0.13	54.5	0.1
DD		0	8.2	29.0	9.1	29.2	5.7	0.018	0.023	10.3	0.13	43.1	0.7
SW		0	8.1	29.0	14.6	25.7	5.2	0.011	0.018	15.7	0.20	40.8	0.0
KC		0	7.2	29.0	11.7	26.4	4.8	0.008	0.016	9.4	0.11	68.9	0.1
MK		0	8.2	29.0	11.3	27.1	4.8	0.013	0.019	49.1	0.87	47.8	0.6
KB		18	8.4	29.0	10.5	25.8	7.6	0.031	0.011	27.0	0.24	51.3	0.0
JK		20	8.2	29.0	10.5	29.7	7.5	0.025	0.014	20.7	0.23	63.8	0.1

Temp = temperature, M.S. = mean size. M.C. = moisture content, TOC = total organic carbon. <sup>a</sup> and <sup>b</sup> indicate overlying water and sediment samples.

denitrification to total N<sub>2</sub> production was calculated by Eq. (5)

$$R_{\text{denitrification}} = D_t / (D_t + A_{29}) \tag{5}$$

where R<sub>denitrification</sub> denotes the contribution of denitrification to total N<sub>2</sub> production.

#### 2.4. DNA isolation, PCR amplification, and sequencing

The extraction of total genomic DNA from approximately 0.25 g sediment from each sampling site was performed using Powersoil™ DNA isolation Kits (MOBIO, USA), as followed by manufacturer's instructions. Subsequently, the DNA extractions were quantified on a

Nano-Drop 2000 spectrophotometer (Thermo USA). The *nirS* gene denitrifier (400 bp) fragments were amplified with primer set of cd3aF (5'-GTSAACGTSAAAGGARACSGG-3') and R3cd (5'-GASTTCGGRTGSGT-CTTGA-3') (Michotey et al., 2000; Throbäck et al., 2004). Polymerase Chain Reaction (PCR) was performed in a total volume of 50  $\mu$ L containing 25  $\mu$ L of Taq PCR Master Mix (including Taq DNA polymerase,  $MgCl_2$ , dNTP, PCR stabilizers, PCR buffer, gel loading reagent and dye; Sangon, China), 1  $\mu$ L DNA (approximately  $10\text{ ng } \mu\text{L}^{-1}$ ), 1  $\mu$ L each of the forward and reverse primer (10  $\mu$ M, Sangon), and 22  $\mu$ L of sterilized  $ddH_2O$ . PCR amplifications were performed under a thermal cycling condition of 95  $^\circ$ C for 4 min, followed by 35 cycles of 94  $^\circ$ C for 30 s, 54  $^\circ$ C for 45 s, 72  $^\circ$ C for 1 min, and a final extension at 72  $^\circ$ C for 5 min. The amplified gene fragments were checked by 1.0% gel electrophoresis. Barcode and adaptor sequences were ligated to the 5'-end of the sequencing primers for multiplexing of the samples in the pyrosequencing runs. The PCR products were sequenced using Illumina Miseq sequencing platform after being purified by OMEGA E.Z.N.A. Cycle-Pure Kit (Omega Bio-Tek, Norcross, USA). The raw sequences were firstly processed using Cutadapt (version 1.9.1) to remove tags and primers (Martin, 2011). The paired-end reads were merged using Pandaseq (version 2.7) (Andre et al., 2012). After possible chimera detection, the software Mothur (version 1.35.1) was used to cluster the remaining high-quality sequences into operational taxonomic units (OTUs) at 97% sequence identity (Schloss et al., 2009). For further analyses, OTUs containing < 0.001% of the total sequences were discarded. Taxonomic identification was performed based on FunGene database (<http://fungene.cme.msu.edu/>) and a constructed phylogenetic tree in this study.

## 2.5. Quantitative PCR (qPCR) assay

The extraction of plasmids carrying the target gene fragment from *Escherichia coli* hosts was conducted via Qiagen Miniprep Spin Kit. The original plasmid concentrations were quantified by a Nano-Drop 2000 spectrophotometer (Thermo USA) for standard curve construction. qPCR was performed in triplicate samples and standards by SYBR green method on ABI 7500 Detection System (Applied Biosystems, Canada). The primer set used for *nirS* gene quantification composed of cd3aF (5'-GTSAACGTSAAAGGARACSGG-3') and R3cd (5'-GASTTCGGRTGSGT-CTTGA-3') (approximately 400 bp) (Michotey et al., 2000; Throbäck et al., 2004). The 25  $\mu$ L-qPCR system contained 12.5  $\mu$ L Fermentas Maxima SYBR Green/Rox Master Mix, 1  $\mu$ L DNA sample (approximately  $10\text{ ng } \mu\text{L}^{-1}$ ), each of the forward and reverse primers 1  $\mu$ L (10  $\mu$ M, Sangon), and 9.5  $\mu$ L sterilized  $ddH_2O$ . The qPCR was performed by the following thermal cycling: 50  $^\circ$ C for 2 min, 95  $^\circ$ C for 10 min, followed by 45 cycles of 95  $^\circ$ C for 30 s, 58  $^\circ$ C for 40 s, and 72  $^\circ$ C for 1 min. Negative controls were run to detect any environmental contamination. The final results were expressed in copies per gram of dry sediment. The standard curve was generated using serial dilution of quantified standard plasmid DNA carrying target fragment. The quantification standard curves were obtained by plotting the cycles of threshold ( $C_T$ ) versus the  $\log_{10}$  values of *nirS* gene copy numbers, with strong linear relationship ( $R^2 = 0.9955$ ) and the amplification efficiency (96.16%). The range of the standard curves was  $1.81 \times 10^5$ – $1.81 \times 10^9$  copies  $\mu\text{L}^{-1}$ . The melt curve single peak was observed at 90.6  $^\circ$ C for the standard and samples, representing that the fluorescent indicators obtained from the expected PCR products.

## 2.6. Data analysis

The diversity indicators (Shannon and Simpson indices), species richness (Chao and Ace estimators), and rarefaction curves were calculated via QIIME 1.9.0 (Caporaso et al., 2010). The construction of phylogenetic tree was performed through a neighbor-joining method via MEGA 7.0.21 software (Kumar et al., 2016), whose topological confidence was evaluated based on 1000 bootstrap replicates.

Community classification of *nirS*-harboring denitrifiers was conducted via principal coordinates analysis (PCoA) using QIIME 1.9.0. Canonical corresponding analysis (CCA) was achieved via Canoco (version 4.5) software to reflect the correlation of *nirS*-harboring denitrifier communities with the environmental factors (ter Braak and Šmilauer, 2002). The determination of potential correlations between the dynamics of *nirS*-harboring denitrifiers and environmental factors was achieved via SPSS software (version 19.0). One-way analysis of variance (ANOVA) was subjected to compare the seasonal and spatial variations in the diversity, abundance, and activity of *nirS*-harboring denitrifiers. In the current study, the statistical analyses were considered significant at  $P < 0.05$ .

## 3. Results

### 3.1. *nirS*-harboring denitrifier diversity

The expected fragments of *nirS* gene (approximately 400 bp) were successfully amplified from all the 24 collected samples from the Indus River Estuary, and a total of 920075 sequences were retrieved. All sequence reads were submitted to the National Center for Biotechnology Information (NCBI) under accession SRP230081. Each dataset of the 24 samples was normalized to 798 sequences for further analyses. When a 3% cut-off value was used, a total of 1625 OTUs were obtained, while 153 OTUs were shared among the freshwater, low-salinity, and high-salinity sampling sites, covering 9.4% of the observed OTUs (Fig. S1). The highest *nirS*-harboring bacterial diversity was detected at the higher salinity site SW in winter, whereas the lowest value was observed at the freshwater site US in summer (Table 2). This result was in agreement with the rarefaction analysis (Fig. S2). However, the *nirS* gene diversity indicated a non-significant spatial difference among the freshwater, low-salinity, and high-salinity sampling sites (one-way ANOVA,  $P > 0.05$ ). Nevertheless, a significant seasonal difference of *nirS*-harboring denitrifying bacterial diversity was detected between summer and winter (one-way ANOVA,  $P < 0.05$ ). The estimated

**Table 2**

Bacterial diversity and richness of *nirS* gene in the sediment samples of the Indus River Estuary.

Season	Sample	Ace	Chao	OTUs <sup>a</sup>	Shannon <sup>b</sup>	Simpson	Coverage (%) <sup>c</sup>
Winter	TB	542	419	225	4.5	0.03	84.7
	GQ	711	451	225	4.6	0.02	84.0
	BR	125	125	96	3.7	0.05	96.1
	AR	404	331	197	4.5	0.02	88.0
	US	494	385	173	3.9	0.06	87.8
	JS	754	487	237	4.5	0.03	82.2
	DD	535	373	222	4.8	0.01	85.8
	SW	578	418	267	5.0	0.01	83.3
	KC	572	427	211	4.4	0.04	85.2
	MK	391	276	173	4.0	0.05	89.0
	KB	429	241	129	3.8	0.04	91.4
	JK	276	217	139	3.6	0.07	92.0
	Summer	TB	121	107	75	3.2	0.07
GQ		278	245	98	3.6	0.04	93.9
BR		286	256	137	3.9	0.05	92.0
AR		340	202	113	2.9	0.17	92.1
US		86	119	59	1.6	0.53	96.9
JS		494	453	251	4.6	0.02	82.0
DD		377	205	89	3.0	0.12	93.6
SW		256	247	172	4.4	0.02	91.1
KC		445	309	158	3.6	0.10	88.8
MK		560	313	130	3.6	0.06	90.4
KB		472	325	174	4.0	0.05	88.2
JK	202	200	149	4.3	0.02	93.5	

<sup>a</sup> OTUs were defined at a similarity of 97%.

<sup>b</sup> Shannon diversity index. A higher number represents more diversity.

<sup>c</sup> Calculated as  $1 - n/N$ , where n is the number of singleton phylotypes and N is the total number of sequences in the sample.

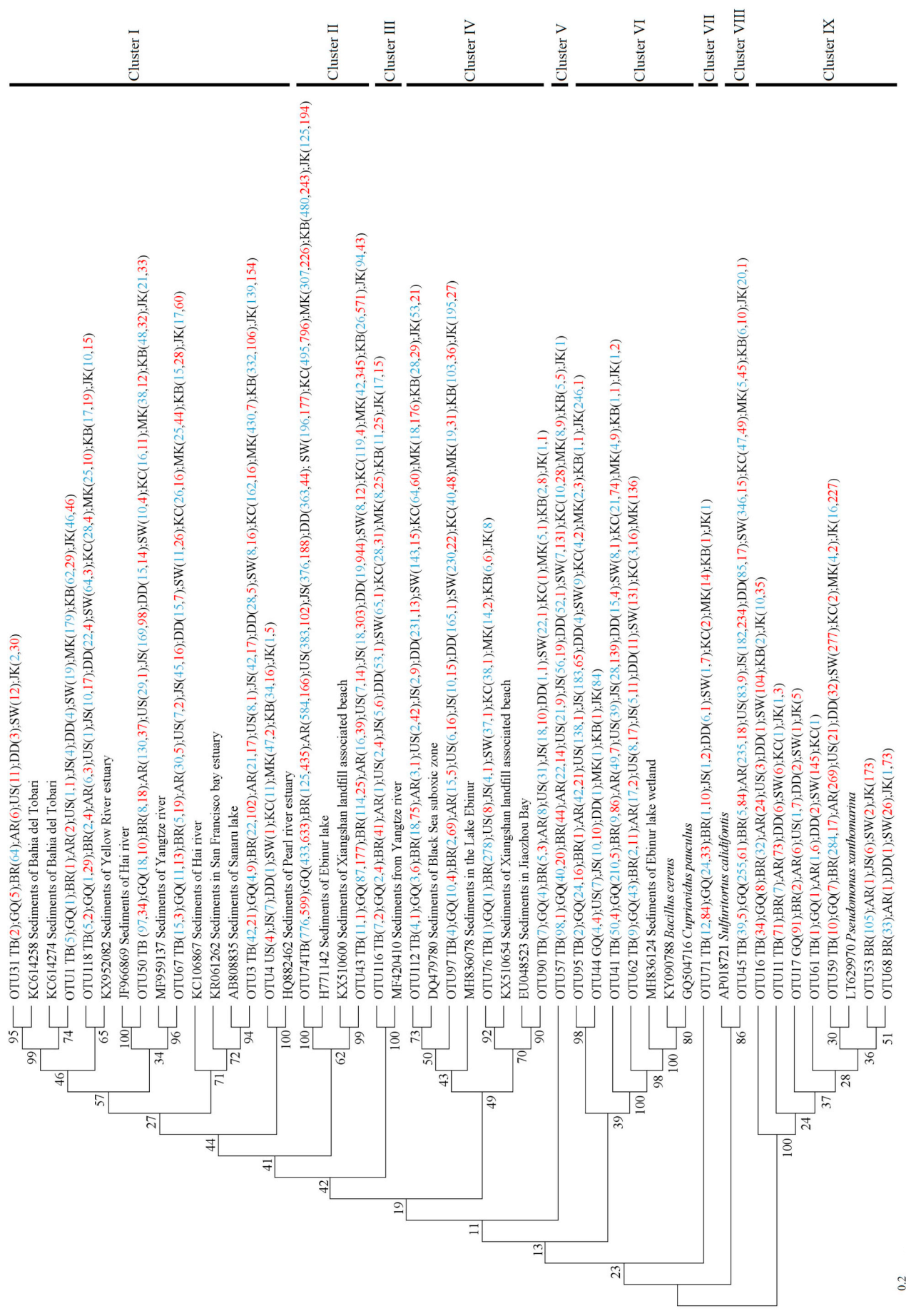


**Fig. 2.** Neighbor-joining phylogenetic tree of *nifS* sequences derived from the intertidal marshes of the Indus River Estuary. OTUs here were defined at 25% nucleotide acid divergence, and the top 28 OTUs (higher than 90% coverage) were chosen for the phylogenetic tree construction. Bootstrap values of 1000 resamplings are shown near nodes. The scale indicates the number of nucleotide substitutions per site. GenBank accession numbers are shown for sequences from other studies. Numbers in parentheses following each site name indicate the number of sequences recovered from each sampling site in summer (red) and winter (blue). (For interpretation of the references to color in this figure legend, the reader is referred to the web version of this article.)

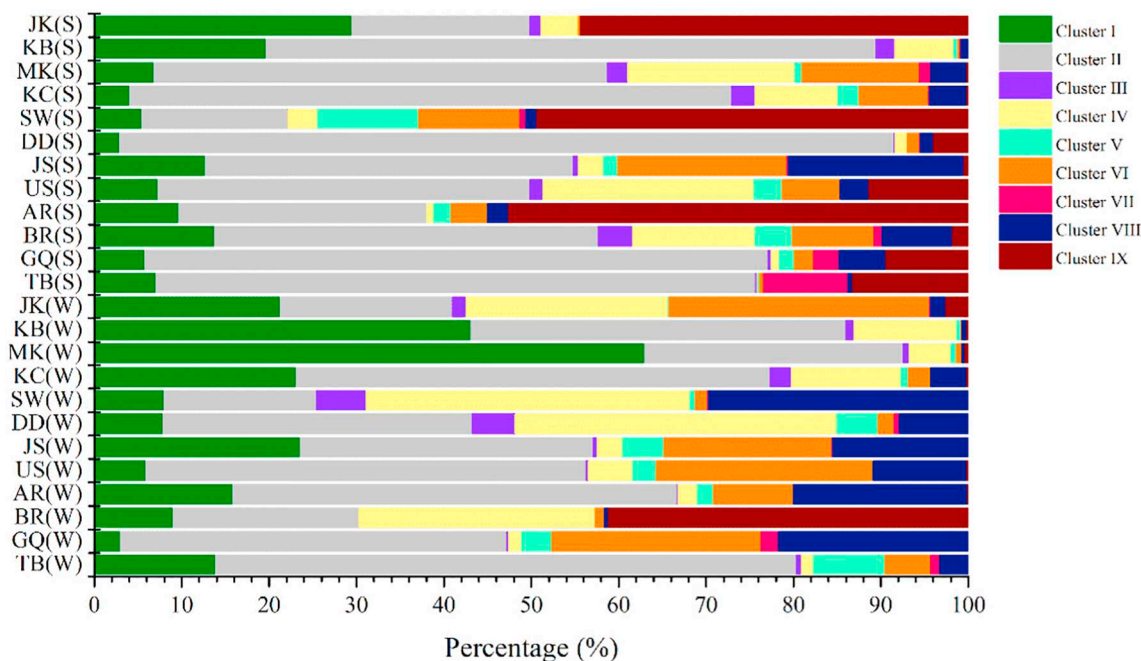


Fig. 3. The community compositions and distributions of *nirS*-harboring denitrifiers in intertidal sediments of the Indus River Estuary.

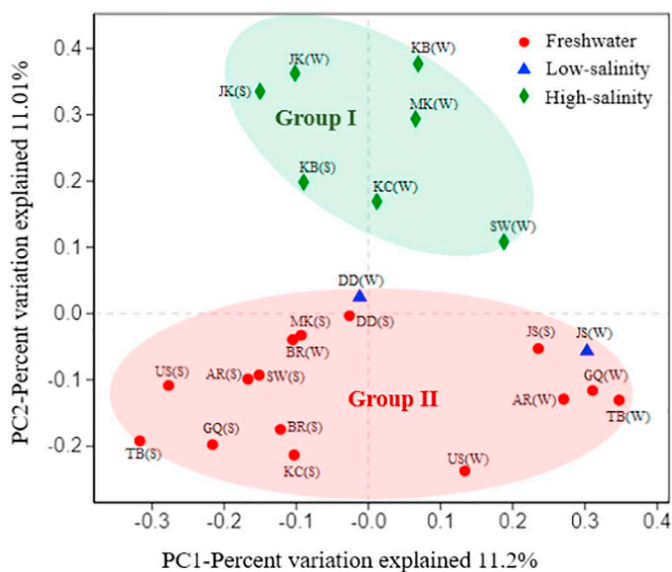


Fig. 4. PCoA analysis of *nirS*-harboring denitrifier communities. The first two principal coordinate axes (PC1–PC2) are shown. W and S represent winter and summer samples, respectively. Group I represents the high-salinity sites. Group II represents the freshwater and low-salinity sites. Red circle, blue triangle, and green diamond symbols represent samples from the freshwater (0 ppt), lower-salinity (11 to 12 ppt), and higher salinity (18 to 36 ppt) sites, respectively. (For interpretation of the references to color in this figure legend, the reader is referred to the web version of this article.)

coverage of the *nirS* gene library ranged from 82.0 to 96.9%, showing that the majority of the *nirS*-type denitrifier genotypes were captured in the present study (Table 2).

### 3.2. Phylogenetic analyses

On the basis of the evolutionary distance, the obtained sequences from the Indus River Estuary were grouped into 9 broadly defined clusters (I–IX) (Fig. 2). They were closely allied with *nirS* genes recovered from the Bahia del Tobarí (KC614258, KC614274) (Beman,

2014), Yellow River Estuary (KX952082) (Li et al., 2017), Hai River (JF966869), Yangtze River (MF959137; MF420410) (Zheng et al., 2015; Jiang et al., 2017), Pearl River Estuary (HQ882462), Jiaozhou Bay (EU048523) (Dang et al., 2009), Lake Sanaru (AB808835), Black Sea suboxic zone (DQ479780) (Oakley et al., 2007), as well as *nirS* gene sequences obtained from landfill beach (KX510600; KX510654). In addition, part of the *nirS* sequences obtained from the Indus River Estuary were closely affiliated with the cultivated denitrifier *Bacillus cereus* (KY090788) (Rout et al., 2017), *Cupriavidus pauculus* (GQ504716), *Pseudomonas xanthomarina* (LT629970), and *Sulfuritortus calidifontis* (AP018721) (Watanabe et al., 2019).

In the sediments of the Indus River Estuary, the *nirS*-harboring denitrifiers in Cluster I were more dominant at the high-salinity habitats (averagely accounting for 29.7% of the retrieved *nirS* sequences in each sample) than at the low-salinity and freshwater sites (averagely accounting for 9.1%) (Fig. 3). Actually, the relative abundance of the cluster I denitrifiers was significantly and positively correlated with salinity ( $P < 0.01$ ). Cluster II occurred in all the 24 collected samples (accounting for 16.6–88.6%), and it harbored the utmost ubiquitous and dominant *nirS*-type denitrifiers of the Indus River Estuary (Fig. 3). In contrast to Cluster I, the *nirS* sequences in Cluster II tended to be more dominant at the freshwater habitats (averagely accounting for 50.4%) than the saline habitats (averagely accounting for 35.9%) (Fig. 3). A similar distribution pattern of the *nirS* sequences in Cluster V was also observed, although the correlation between their relative abundance and salinity was not significant ( $P > 0.05$ ). The sequences of *nirS* gene in Cluster IX were closely allied with the cultivated denitrifier *Pseudomonas xanthomarina*, and this type of denitrifier was mainly found in the summer samples, which averagely accounting for 15.6% and 3.7% of the *nirS*-harboring denitrifiers in summer and winter, respectively. In the Indus River estuarine surface sediments, most of the denitrifying bacterial sequences (averagely accounting for 62.9% of the overall *nirS* sequences) were unclassified bacteria at the family level (Fig. S3).

### 3.3. Distribution of *nirS*-harboring denitrifiers

The spatial and seasonal distributions of the *nirS*-type denitrifier communities in the Indus River Estuary were determined by PCoA

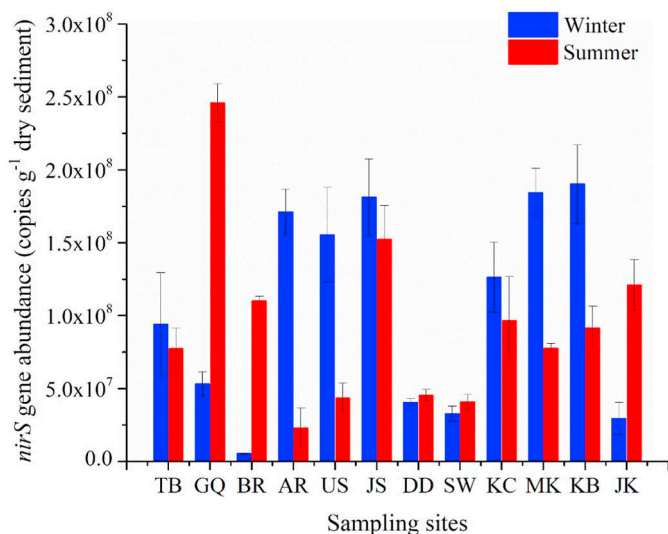


**Fig. 5.** The abundance of *nirS* gene denitrifiers in the sediments of the Indus River Estuary. Vertical bars indicate standard deviation ( $n = 3$ ).

analyses (Fig. 4). The first two principle coordinate axes (PC1 and PC2) described 22.21% of the cumulative variance in the *nirS*-harboring denitrifiers. Based on these two principle coordinate axes, the *nirS*-harboring denitrifier communities were divided into two separated groups (Fig. 4). Group I was retrieved in the high-salinity sediments (16–36 ppt), whereas those in group II were recovered in the low-salinity and freshwater sediments (0–15 ppt). However, no significant seasonal difference in the distribution of *nirS*-type denitrifier communities was detected in the sediments of the Indus River Estuary (Fig. 4).

### 3.4. Quantification of *nirS*-harboring denitrifiers

qPCR showed that the *nirS* gene copy numbers ranged from  $5.3 \times 10^6$  to  $1.9 \times 10^8$  copies  $g^{-1}$  dry sediment in winter and from  $2.3 \times 10^7$  to  $2.5 \times 10^8$  copies  $g^{-1}$  dry sediment in summer in the sediments of the Indus River Estuary (Fig. 5). The highest *nirS* gene copy number ( $2.5 \times 10^8$  copies  $g^{-1}$  dry sediment) was found at site GQ in summer, and the lowest *nirS* gene copy number ( $5.3 \times 10^6$  copies  $g^{-1}$  dry sediment) was observed at site BR in winter. The average *nirS* gene copy number was higher at the saline regions ( $9.3 \times 10^7$  copies  $g^{-1}$  dry sediment) than at the freshwater sites ( $2.2 \times 10^8$  copies  $g^{-1}$  dry sediment), but no significant spatial difference was observed (one-way ANOVA,  $P > 0.05$ ). Although the seasonal variation was not significant (one-way ANOVA,  $P > 0.05$ ), the abundance of *nirS*-type denitrifiers tended to be higher in winter than in summer, with average values of  $1.1 \times 10^8$  and  $9.4 \times 10^7$  copies  $g^{-1}$  dry sediment, respectively.

### 3.5. Denitrification rates

Slurry incubations were performed with a  $^{15}N$  tracing technique, and the production of  $^{15}N$ -labelled  $N_2$  from the incubations amended with  $^{15}NO_3^-$  was used to determine the denitrification rates in the estuarine environment. The estimated denitrification rates ranged from 0.01 to  $6.27 \mu mol N kg^{-1} h^{-1}$  in the sediments of the Indus River Estuary (Fig. 6). In this study, although there was no significant seasonal variation of denitrification rate (one-way ANOVA,  $P > 0.05$ ), denitrifiers tended to be more active in winter than in summer, with average values of 1.9 and  $1.2 \mu mol N kg^{-1} h^{-1}$ , respectively. Along the Indus River Estuary, no significant spatial variation of denitrification rates was observed among different salinity levels in winter (one-way ANOVA,  $P > 0.05$ ). However, the denitrification rates were significantly higher at the saline sites than at the freshwater-dominated

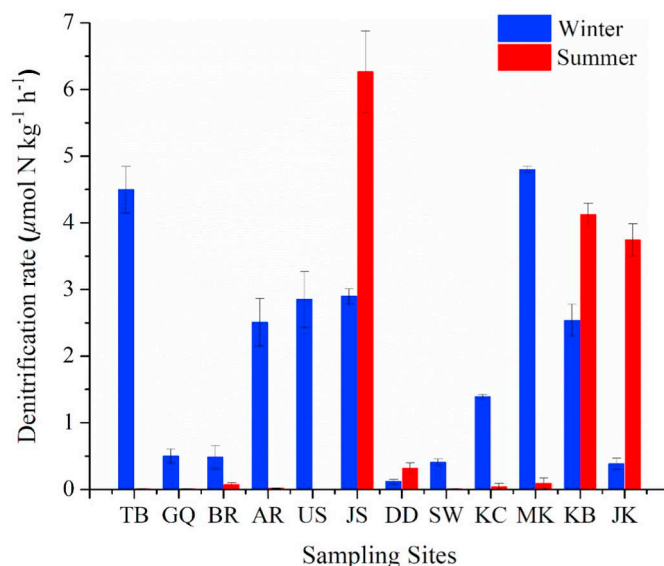


**Fig. 6.** The spatiotemporal variations of denitrification rates in the sediments of the Indus River Estuary in winter and summer, respectively. Vertical bars indicate standard deviation ( $n = 3$ ).

sites in summer (except site JS), with average values of 3.9 and  $0.1 \mu mol N kg^{-1} h^{-1}$ , respectively ( $P < 0.05$ ).

### 3.6. Relationships of *nirS*-harboring denitrifier communities, abundance, and activity with environmental factors

Canonical correspondence analysis (CCA) was performed to determine the potential effect of environmental factors on the *nirS*-harboring denitrifier communities (Fig. 7). The first two CCA axes (CCA1 and CCA2) explained 12.34% of the cumulative variance of the *nirS*-harboring denitrifier genotype-environment relationship. The results revealed significant correlations of *nirS*-harboring denitrifier community structure with TOC, Fe(III), moisture content, and  $NO_3^-$  ( $P < 0.05$ ), however other environmental factors (temperature, pH, salinity, mean size, sulfide, Fe(II),  $NO_2^-$ , and  $NH_4^+$ ) were not correlated significantly ( $P > 0.05$ ) (Fig. 7). In addition, the correlation of *nirS*-harboring denitrifier diversity with environmental factors was analyzed by SPSS 19.0 software. The diversity of *nirS*-harboring denitrifier was negatively correlated with temperature ( $R = -0.532$ ,  $P = 0.007$ ) (Table S1). In addition, the abundance of *nirS* gene was correlated significantly with  $NO_3^-$  content in the sediment ( $R = 0.421$ ,  $P = 0.040$ ) (Table S2). Furthermore, denitrification rates were correlated significantly with TOC ( $R = 0.438$ ,  $P = 0.032$ ) and Fe(II) ( $R = 0.523$ ,  $P = 0.009$ ) (Table S3). A significant and positive linear relationship was detected between denitrification rates and the associated *nirS* gene abundance in the surface sediments of Indus River Estuary ( $P < 0.05$ ) (Fig. S4).

## 4. Discussion

Nowadays, the Indus River faces severe water pollution because of excessive nitrogen inputs from human activities, and consequently the excessive nitrogen is transported by rivers to seas, causing coastal eutrophication (Kravtsova et al., 2009; Kidwai et al., 2019; Wang et al., 2019). Therefore, it is of great significance to deep understand the microbial reactive nitrogen removal process in the Indus River Estuary. To the best of our knowledge, this is the first study to examine the *nirS*-harboring denitrifier community diversity, abundance, activity, and distribution in the sediments of the Indus River Estuary. The biodiversity of *nirS*-harboring denitrifiers obtained in the Indus River Estuary was approximate to those previously described in other environments,

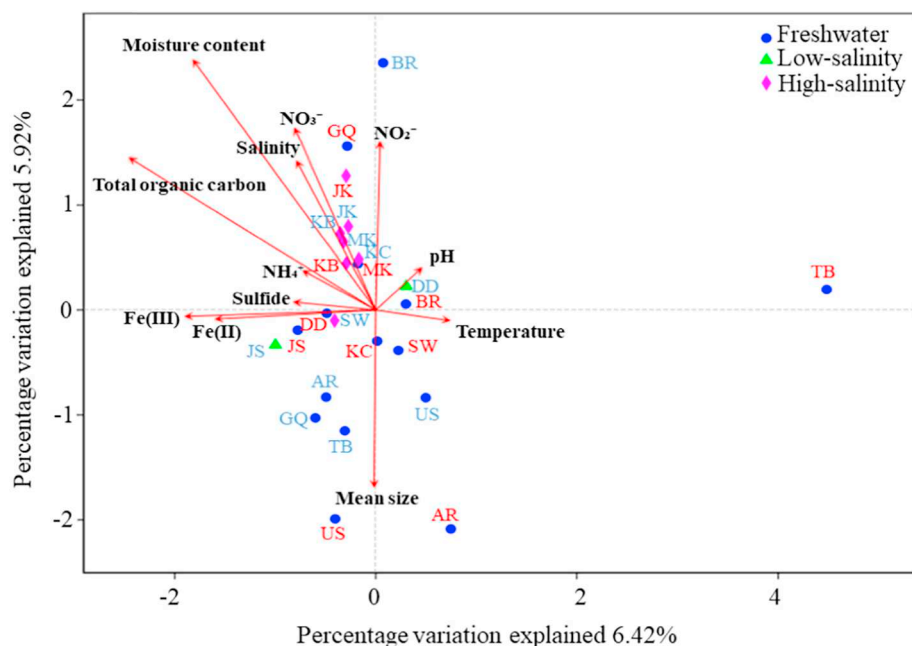


Fig. 7. Canonical correspondence analysis (CCA) ordination plots for the first two principal dimensions of the relationship between *nirS*-harboring denitrifier communities with the environmental parameters. Blue and Red font represent winter and summer sites, respectively. Circle, triangle, and diamond symbols represent freshwater, low-salinity, and high-salinity sites, respectively. (For interpretation of the references to color in this figure legend, the reader is referred to the web version of this article.)

such as the Chesapeake Bay Estuary, Jiaozhou Bay, and freshwater lakes (Dang et al., 2009; Francis et al., 2013; Guo et al., 2014). The sequences of *nirS*-harboring denitrifier retrieved from the Indus River Estuary showed high identity with those from other estuarine and coastal environments, like the Yellow River Estuary, Pearl River Estuary, and the Yangtze River Estuary (Fig. 2) (Li et al., 2017; Jiang et al., 2017; Zheng et al., 2015). But, the communities of *nirS*-type denitrifiers in the Indus River Estuary were significantly different from those obtained from the above estuarine ecosystems and other coastal wetlands of China (Fig. S5) (Gao et al., 2016). Furthermore, the dominant *nirS* genotypes observed in the Indus River Estuary are affiliated with unclassified denitrifying bacteria (Fig. S3). This result implies that we still have very limited knowledge about denitrifiers in the estuarine ecosystems.

Recent results showed that salinity may be a vital factor for the distribution and activity of denitrifiers (Zheng et al., 2015; Bai et al., 2017). In the Yangtze River estuarine intertidal marshes, the *nirS*-harboring denitrifier communities had distinctive spatial variation along the salinity gradient (Zheng et al., 2015). In the present study, a similar distribution pattern of *nirS*-harboring denitrifiers was observed in the Indus River Estuary, where the denitrifier communities were divided into two different groups (Fig. 4). Group I was retrieved in the high-salinity sediments, whereas those in group II were recovered in the low-salinity and freshwater sediments (Fig. 4). These results further confirmed that salinity may play a crucial role in regulating the biogeographical distribution of *nirS*-harboring denitrifiers in estuarine environments. This statement was also strengthened by the CCA in the present study (Fig. 7). In addition to salinity, the environmental factors including moisture content, TOC,  $\text{NO}_3^-$ , and Fe(II) could also influence the denitrification process (Bai et al., 2017; Cheng et al., 2016; Deng et al., 2015; Shan et al., 2016). Moisture content was reported to positively correlate with the activity of denitrifiers (Bai et al., 2017; Ruser et al., 2006), as the increase of soil moisture leads to lower oxygen which might facilitate the process of denitrification (Smith, 1980). However, no significant correlation was observed between denitrification rates and moisture content in the present study ( $P > 0.05$ ). Nevertheless, moisture content was observed to significantly correlate with the distribution of the *nirS*-encoding denitrifiers in the marsh sediments of the Indus River Estuary ( $P < 0.05$ ), which suggested that different micro-environment caused by diverse sediment water content might lead to different denitrifier communities.

The presence of TOC enhanced the reduction of  $\text{NO}_3^-$  in an anoxic environment (Deng et al., 2015; Rahman et al., 2019). Organic carbon has been reported to promote the process of denitrification, which was consistent with our results (Cheng et al., 2016; Deng et al., 2015; Jia et al., 2016).  $\text{NO}_3^-$  is also an important substrate for the denitrification process, and it has a crucial role in regulation of the activity of denitrifiers (Dunn et al., 2013; Roberts et al., 2012; Yu et al., 2013). In the Indus River Estuary,  $\text{NO}_3^-$  was observed to significantly correlate with the distribution and abundance of the *nirS*-harboring denitrifiers (Fig. 7 and Table S2). In addition, a large number of chemoheterotrophic microorganisms are able to utilize Fe(II) as reductant for  $\text{NO}_3^-$  reduction, instead of utilizing organic matter (Ottley et al., 1997; Straub et al., 1996). Actually, microbial  $\text{NO}_3^-$ -dependent Fe(II) oxidation was determined in freshwater environment as well as hypersaline environment (Emmerich et al., 2012; Weber et al., 2006). Previous studies showed that iron was an important environmental factor affecting the activity of denitrifiers (Baeseaman et al., 2006; Cheng et al., 2016), and this point was confirmed in the current study as a significant correlation was observed between the potential denitrification rates and Fe(II). In addition, the community structure of *nirS*-harboring denitrifiers was correlated significantly with Fe(III) in the Indus River Estuary. Furthermore, pH was considered as one of the main environmental variables affecting the community structure and dynamics of denitrifiers (Čuhel and Šimek, 2011; Yang et al., 2018). However, in this study, pH was not significantly correlated with the biodiversity, abundance, and activity of *nirS*-harboring denitrifiers. Similarly, there was also no significant correlation between pH and the *nirS*-harboring denitrifier community dynamics in the intertidal sediments of the Yangtze Estuary (Zheng et al., 2015).

The *nirS* gene abundance ranged from  $5.3 \times 10^6$  to  $2.5 \times 10^8$  copies  $\text{g}^{-1}$  dry sediment in the sediments of the Indus River Estuary, which was approximate to those determined in the sediments of the Yangtze estuary ( $1.01 \times 10^6$  to  $9.00 \times 10^7$  copies  $\text{g}^{-1}$  sediment) (Zheng et al., 2015), created riverine wetland ( $6.8 \times 10^7$  to  $3.4 \times 10^9$  copies  $\text{g}^{-1}$  sediment) (Ligi et al., 2014), and Bahia del Tobarí estuary ( $2.72 \times 10^6$  to  $8.82 \times 10^7$  copies  $\text{g}^{-1}$  sediment) (Beman, 2014), but was comparatively higher than those measured in the Laizhou bay sediments ( $8.67 \times 10^5$  to  $5.68 \times 10^6$  copies  $\text{g}^{-1}$  sediment) (Wang et al., 2014) and the paddy field soil ( $6.0 \times 10^5$  to  $1.2 \times 10^6$  copies  $\text{g}^{-1}$  soil) (Yoshida et al., 2009). The *nirS* gene abundance was only correlated significantly with  $\text{NO}_3^-$  content

( $P < 0.05$ ). In addition, a previous reports also mentioned that sulfide could influence the growth of *nirS*-harboring denitrifiers (Aelion and Warttinger, 2010; Sorensen et al., 1980). However, no significant correlation was detected between sulfide and the abundance and activity of denitrifiers in the present study. The *nirS* gene abundance was slightly higher in winter than in summer, while no significant seasonal difference was observed (one-way ANOVA,  $P > 0.05$ ). In addition, the denitrification rates also showed no significant seasonal variation in the sediments of the Indus River Estuary (one-way ANOVA,  $P > 0.05$ ). These results might be due to the relatively weaker seasonal difference in temperature in the Indus River Estuary (approximately 10 °C).

Compared with anammox, it is estimated that the denitrification process averagely contributed 78.1% to the total nitrogen loss in the marsh sediments of the Indus River Estuary, which was comparable to those detected in other aquatic ecosystems, such as the Yangtze Estuary (38–96%) (Deng et al., 2015), the East China Sea (17–85%) (Song et al., 2013), and the Arabian Sea (87–99%) (Ward et al., 2009). If the measured potential denitrification rates were extrapolated to the entire delta area, approximately  $7.2 \times 10^5$  t nitrogen can be removed annually by denitrifiers. This potential nitrogen-removal amount accounts for about 20% of the total nitrogen inputs to the Indus basin (Wang et al., 2019). Therefore, denitrification plays an important role in alleviating coastal water pollution, especially considering that the nitrogen inputs will continue to increase due to the population growth, economic development, and climate change in the future (Wang et al., 2019). It was reported that there was a wide discharge of heavy metals (e.g., Cu and Pb) in the Indus River, and the accumulation of heavy metals might have severe effect on bacterial biodiversity, abundance, and activity (Gans et al., 2005; Tariq et al., 1996; Yao et al., 2017). However, the heavy metals were not measured in the present study, and their potential effects on denitrification process will be addressed in our future research.

In summary, this work investigated the abundance, biodiversity, distribution of *nirS*-harboring denitrifiers and the potential denitrification rates in the sediments of the Indus River Estuary. The denitrification rates ranged from 0.01 to 6.27  $\mu\text{mol N kg}^{-1} \text{h}^{-1}$  and the abundance of *nirS* gene ranged from  $5.3 \times 10^6$  to  $2.5 \times 10^8$  copies  $\text{g}^{-1}$  dry sediment. Along the salinity gradient of the Indus River Estuary, *nirS*-harboring denitrifier communities exhibited distinctive spatial heterogeneity, however, the abundance and activity of *nirS*-harboring denitrifiers indicated a non-significant spatiotemporal variation. The denitrification process was an important nitrogen removal pathway in the Indus River Estuary, which can help to alleviate the coastal water pollution and harmful algae blooms. These results provide novel insights into the community dynamics and important role of denitrifiers in estuarine ecosystems.

#### CRediT authorship contribution statement

**Fozia:** Formal analysis, Investigation, Data curation, Writing - original draft. **Yanling Zheng:** Conceptualization, Formal analysis, Writing - review & editing. **Lijun Hou:** Conceptualization, Methodology, Writing - review & editing. **Zongxiao Zhang:** Methodology, Formal analysis. **Dengzhou Gao:** Methodology. **Guoyu Yin:** Investigation. **Ping Han:** Validation. **Hongpo Dong:** Methodology. **Xia Liang:** Methodology. **Yi Yang:** Resources. **Min Liu:** Conceptualization, Funding acquisition.

#### Declaration of competing interest

The authors declare that they have no conflict of interest.

#### Acknowledgments

This work is funded by National Natural Science Foundation of China (Nos. 41725002, 41671463, 41761144062, 41730646,

41601530, and 41971105). It is also supported by Chinese National Key Programs for Fundamental Research and Development (No. 2016YFA0600904 and 2016YFE0133700), and the Yangtze Delta Estuarine Wetland Station, East China Normal University. Gene sequence data in this paper can be downloaded from National Center for Biotechnology Information (NCBI) under accession SRP230081, and other data can be obtained by sending a written request to the corresponding author.

#### Appendix A. Supplementary data

Supplementary data to this article can be found online at <https://doi.org/10.1016/j.marpolbul.2020.110971>.

#### References

- Aelion, C.M., Warttinger, U., 2010. Sulfide inhibition of nitrate removal in coastal sediments. *Estuar. Coasts* 33, 798–803.
- Ali, K.F., de Boer, D.H., 2008. Factors controlling specific sediment yield in the upper Indus River basin, northern Pakistan. *Hydrol. Process.* 22, 3102–3114.
- Amin, M.N., Kroeze, C., Strokal, M., 2017. Human waste: an underestimated source of nutrient pollution in coastal seas of Bangladesh, India and Pakistan. *Mar. Pollut. Bull.* 118, 131–140.
- An, S., Gardner, W.S., 2002. Dissimilatory nitrate reduction to ammonium (DNRA) as a nitrogen link, versus denitrification as a sink in a shallow estuary (Laguna Madre/Baffin Bay, Texas). *Mar. Ecol. Prog. Ser.* 237, 41–50.
- Andre, P.M., Andrea, K.B., Jakub, M.T., Daniel, G.B., Josh, D.N., 2012. PANDAseq: paired-end assembler for illumina sequences. *BMC Bioinformatics* 13, 31.
- Baeseman, J.L., Smith, R.L., Silverstein, J., 2006. Denitrification potential in stream sediments impacted by acid mine drainage: effects of pH, various electron donors, and iron. *Microb. Ecol.* 51, 232–241.
- Bai, J., Wang, X., Jia, J., Zhang, G., Wang, Y., Zhang, S., 2017. Denitrification of soil nitrogen in coastal and inland salt marshes with different flooding frequencies. *Phys. Chem. Earth* 97, 31–36.
- Beman, J.M., 2014. Activity, abundance, and diversity of nitrifying archaea and denitrifying bacteria in sediments of a subtropical estuary: Bahía del Tóbari, Mexico. *Estuar. Coasts* 37, 1343–1352.
- Booth, M.S., Campbell, C., 2007. Spring nitrate flux in the Mississippi River Basin: a landscape model with conservation applications. *Environ. Sci. Technol.* 41, 5410–5418.
- ter Braak, C.J.F., Šmilauer, P., 2002. CANOCO Reference Manual and CanoDraw for Windows User's Guide: Software for Canonical Community Ordination (Version 4.5). Microcomputer Power, Ithaca, NY.
- Caporaso, J.G., Kuczynski, J., Stombaugh, J., Bittinger, K., Bushman, F.D., Costello, E.K., Fierer, N., Pena, A.G., Goodrich, J.K., Gordon, J.L., Huttley, G.A., Kelley, S.T., Knights, D., Koenig, J.E., Ley, R.E., Lozupone, C.A., McDonald, D., Muegge, B.D., Pirrung, M., Reeder, J., Sevinsky, J.R., Turnbaugh, P.J., Walters, W.A., Widmann, J., Yatsunenko, T., Zaneveld, J., Knight, R., Peña, A.G., Goodrich, J.K., Gordon, J.L., Huttley, G.A., Kelley, S.T., Knights, D., Koenig, J.E., Ley, R.E., Lozupone, C.A., McDonald, D., Muegge, B.D., Pirrung, M., Reeder, J., Sevinsky, J.R., Turnbaugh, P.J., Walters, W.A., Widmann, J., Yatsunenko, T., Zaneveld, J., Knight, R., 2010. QIIME allows analysis of high-throughput community sequencing data. *Nat. Methods* 7, 335–336.
- Cheng, L., Li, X., Lin, X., Hou, L., Liu, M., Li, Y., Liu, S., Hu, X., 2016. Dissimilatory nitrate reduction processes in sediments of urban river networks: spatiotemporal variations and environmental implications. *Environ. Pollut.* 219, 545–554.
- Cline, J.D., 1969. Spectrophotometric determination of hydrogen sulfide in natural waters. *Limnol. Oceanogr.* 14, 454–458.
- Coyne, M.S., Arunakumari, A., Averill, B.A., Tiedje, J.M., 1989. Immunological identification and distribution of dissimilatory heme cd<sub>1</sub> and nonheme copper nitrite reductases in denitrifying bacteria. *Appl. Environ. Microbiol.* 55, 2924–2931.
- Čuhel, J., Šimek, M., 2011. Proximal and distal control by pH of denitrification rate in a pasture soil. *Agric. Ecosyst. Environ.* 141, 230–233.
- Dalsgaard, T., Thamdrup, B., Fariás, L., Revsbech, N.P., 2012. Anammox and denitrification in the oxygen minimum zone of the eastern South Pacific. *Limnol. Oceanogr.* 57, 1331–1346.
- Dang, H., Wang, C., Li, J., Li, T., Tian, F., Jin, W., Ding, Y., Zhang, Z., 2009. Diversity and distribution of sediment *nirS*-encoding bacterial assemblages in response to environmental gradients in the eutrophied Jiaozhou Bay, China. *Microb. Ecol.* 58, 161–169.
- Davidson, N.C., 2016. Indus waters treaty. In: *The Wetland Book*, pp. 1–4.
- Deegan, L.A., Johnson, D.S., Warren, R.S., Peterson, B.J., Fleeger, J.W., Fagherazzi, S., Wollheim, W.M., 2012. Coastal eutrophication as a driver of salt marsh loss. *Nature* 490, 388–392.
- Deng, F., Hou, L., Liu, M., Zheng, Y., Yin, G., Li, X., Lin, X., Chen, F., Gao, J., Jiang, X., 2015. Dissimilatory nitrate reduction processes and associated contribution to nitrogen removal in sediments of the Yangtze Estuary. *Journal of Geophysical Research G: Biogeosciences* 120, 1521–1531.
- Diaz, R.J., Rosenberg, R., 2008. Spreading dead zones and consequences for marine ecosystems. *Science* 321, 926–929.
- Dunn, R.J.K., Robertson, D., Teasdale, P.R., Waltham, N.J., Welsh, D.T., 2013. Benthic metabolism and nitrogen dynamics in an urbanised tidal creek: domination of DNRA over denitrification as a nitrate reduction pathway. *Estuar. Coast. Shelf Sci.* 131, 271–281.

- Emmerich, M., Bhansali, A., Lösekann-Behrens, T., Schröder, C., Kappler, A., Behrens, S., 2012. Abundance, distribution, and activity of Fe(II)-oxidizing and Fe(III)-reducing microorganisms in hypersaline sediments of Lake Kasin, Southern Russia. *Appl. Environ. Microbiol.* 78, 4386–4399.
- Fowler, D., Coyle, M., Skiba, U., Sutton, M.A., Cape, J.N., Reis, S., Sheppard, L.J., Jenkins, A., Grizzetti, B., Galloway, J.N., Vitousek, P., Leach, A., Bouwman, A.F., Butterbach-Bahl, K., Dentener, F., Stevenson, D., Amann, M., Voss, M., 2013. The global nitrogen cycle in the twenty-first century. *Philosophical Transactions of the Royal Society B: Biological Sciences* 368.
- Francis, C.A., O'Mullan, G.D., Cornwell, J.C., Ward, B.B., 2013. Transitions in nirS-type denitrifier diversity, community composition, and biogeochemical activity along the Chesapeake Bay estuary. *Front. Microbiol.* 4.
- Galloway, J.N., 2013. The global nitrogen cycle. *Treatise on Geochemistry: Second Edition* 10, 475–498.
- Galloway, J.N., Dentener, F.J., Capone, D.G., Boyer, E.W., Howarth, R.W., Seitzinger, S.P., Asner, G.P., Cleveland, C.C., Green, P.A., Holland, E.A., Karl, D.M., Michaels, A.F., Porter, J.H., Townsend, A.R., Vörösmarty, C.J., 2004. Nitrogen cycles: past, present, and future. *Biogeochemistry* 70, 153–226.
- Galloway, J.N., Townsend, A.R., Erisman, J.W., Bekunda, M., Cai, Z., Freney, J.R., Martinelli, L.A., Seitzinger, S.P., Sutton, M.A., 2008. Transformation of the nitrogen cycle: recent trends, questions, and potential solutions. *Science* 320, 889–892.
- Gans, J., Wolinsky, M., Dunbar, J., 2005. Microbiology: computational improvements reveal great bacterial diversity and high toxicity in soil. *Science* 309, 1387–1390.
- Gao, J., Hou, L.J., Zheng, Y.L., Liu, M., Yin, G.Y., Li, X.F., Lin, X.B., Yu, C.D., Wang, R., Jiang, X.F., Sun, X.R., 2016. nirS-encoding denitrifier community composition, distribution, and abundance along the coastal wetlands of China. *Appl. Microbiol. Biotechnol.* 100, 8573–8582.
- Glibert, P.M., Anderson, D.M., Gentien, P., Granéli, E., Sellner, K.G., 2005. The global, complex phenomena of harmful algal blooms. *Oceanography* 18, 136–147.
- Glockner, A.B., Jüngst, A., Zumft, W.G., 1993. Copper-containing nitrite reductase from *Pseudomonas aureofaciens* is functional in a mutationally cytochrome *cd1*-free background (nirS) of *Pseudomonas stutzeri*. *Arch. Microbiol.* 160, 18–26.
- Gruber, N., Galloway, J.N., 2008. An earth-system perspective of the global nitrogen cycle. *Nature* 451, 293–296.
- Guo, L., Hu, Z., Fang, F., Liu, T., Chuai, X., Yang, L., 2014. Trophic status determines the nirS-denitrifier community in shallow freshwater lakes. *Ann. Microbiol.* 64, 999–1006.
- Hochstein, L.I., Tomlinson, G.A., 2003. The enzymes associated with denitrification. *Annu. Rev. Microbiol.* 42, 231–261.
- Hou, L., Zheng, Y., Liu, M., Gong, J., Zhang, X., Yin, G., You, L., 2013. Anaerobic ammonium oxidation (anammox) bacterial diversity, abundance, and activity in marsh sediments of the Yangtze Estuary. *J. Geophys. Res. Biogeosci.* 118, 1237–1246.
- Hu, M., Wilson, B.J., Sun, Z., Ren, P., Tong, C., 2017. Effects of the addition of nitrogen and sulfate on CH<sub>4</sub> and CO<sub>2</sub> emissions, soil, and pore water chemistry in a high marsh of the Min River estuary in southeastern China. *Sci. Total Environ.* 579, 292–304.
- Hussain, Z., 2011. Application of the regional flood frequency analysis to the upper and lower basins of the Indus River, Pakistan. *Water Resour. Manag.* 25, 2797–2822.
- Inam, A., Clift, P.D., Giosan, L., Tabrez, A.R., Tahir, M., Rabbani, M.M., Danish, M., 2008. The geographic, geological and oceanographic setting of the Indus River. *Large Rivers: Geomorphology and Management* 333–346.
- Jia, Z., Liu, T., Xia, X., Xia, N., 2016. Effect of particle size and composition of suspended sediment on denitrification in river water. *Sci. Total Environ.* 541, 934–940.
- Jiang, X., Yao, L., Guo, L., Liu, G., Liu, W., 2017. Multi-scale factors affecting composition, diversity, and abundance of sediment denitrifying microorganisms in Yangtze lakes. *Appl. Microbiol. Biotechnol.* 101, 8015–8027.
- Kidwai, S., Ahmed, W., Tabrez, S.M., Zhang, J., Giosan, L., Clift, P., Inam, A., 2019. The Indus Delta—catchment, River, Coast, and People. *Coasts and Estuaries* 213–232.
- Kravtsova, V.I., Mikhailov, V.N., Eferemova, N.A., 2009. Variations of the hydrological regime, morphological structure, and landscapes of the Indus River Delta (Pakistan) under the effect of large-scale water management measures. *Water Resour.* 36, 365–379.
- Kumar, S., Stecher, G., Tamura, K., 2016. MEGA7: molecular evolutionary genetics analysis version 7.0 for bigger datasets. *Mol. Biol. Evol.* 33, 1870–1874.
- Li, F., Li, M., Shi, W., Li, H., Sun, Z., Gao, Z., 2017. Distinct distribution patterns of proteobacterial nirK- and nirS-type denitrifiers in the Yellow River estuary, China. *Can. J. Microbiol.* 63, 708–718.
- Ligi, T., Truu, M., Truu, J., Nölvak, H., Kaasik, A., Mitsch, W.J., Mander, Ü., 2014. Effects of soil chemical characteristics and water regime on denitrification genes (nirS, nirK, and nosZ) abundances in a created riverine wetland complex. *Ecol. Eng.* 72, 47–55.
- Luo, G., Junium, C.K., Izon, G., Ono, S., Beukes, N.J., Algeo, T.J., Cui, Y., Xie, S., Summons, R.E., 2018. Nitrogen fixation sustained productivity in the wake of the palaeoproterozoic great oxygenation event. *Nat. Commun.* 9, 978.
- Martin, M., 2011. Cutadapt removes adapter sequences from high-throughput sequencing reads. *EMBnet. Journal* 17, 10.
- Michotey, V., Méjean, V., Bonin, P., 2000. Comparison of methods for quantification of cytochrome *cd1*-denitrifying bacteria in environmental marine samples. *Appl. Environ. Microbiol.* 66, 1564–1571.
- Oakley, B.B., Francis, C.A., Roberts, K.J., Fuchsman, C.A., Srinivasan, S., Staley, J.T., 2007. Analysis of nitrite reductase (nirK and nirS) genes and cultivation reveal depauperate community of denitrifying bacteria in the Black Sea suboxic zone. *Environ. Microbiol.* 9, 118–130.
- Ottley, C.J., Davison, W., Edmunds, W.M., 1997. Chemical catalysis of nitrate reduction by iron(II). *Geochim. Cosmochim. Acta* 61, 1819–1828.
- Paerl, H.W., 1997. Coastal eutrophication and harmful algal blooms: importance of atmospheric deposition and groundwater as 'new' nitrogen and other nutrient sources. *Limnol. Oceanogr.* 42, 1154–1165.
- Rahman, M.M., Roberts, K.L., Grace, M.R., Kessler, A.J., Cook, P.L.M., 2019. Role of organic carbon, nitrate and ferrous iron on the partitioning between denitrification and DNRA in constructed stormwater urban wetlands. *Sci. Total Environ.* 666, 608–617.
- Roberts, K.L., Eate, V.M., Eyre, B.D., Holland, D.P., Cook, P.L.M., 2012. Hypoxic events stimulate nitrogen recycling in a shallow salt-water estuary: the Yarra River estuary, Australia. *Limnol. Oceanogr.* 57, 1427–1442.
- Roden, E.E., Lovley, D.R., 1993. Evaluation of <sup>55</sup>Fe as a tracer of Fe(III) reduction in aquatic sediments. *Geomicrobiol. J.* 11, 35–48.
- Rout, P.R., Bhunia, P., Dash, R.R., 2017. Simultaneous removal of nitrogen and phosphorus from domestic wastewater using *Bacillus cereus* GS-5 strain exhibiting heterotrophic nitrification, aerobic denitrification and denitrifying phosphorous removal. *Bioresour. Technol.* 244, 484–495.
- Ruser, R., Flessa, H., Russow, R., Schmidt, G., Buegger, F., Munch, J.C., 2006. Emission of N<sub>2</sub>O, N<sub>2</sub> and CO<sub>2</sub> from soil fertilized with nitrate: effect of compaction, soil moisture and rewetting. *Soil Biol. Biochem.* 38, 263–274.
- Saifullah, S.M., Khan, S.H., Ismail, S., 2002. Distribution of nickel in a polluted mangrove habitat of the Indus Delta. *Mar. Pollut. Bull.* 44, 570–576.
- Sakurai, T., Kataoka, K., 2007. Structure and function of type I copper multicopper oxidases. *Cell. Mol. Life Sci.* 64, 2642–2656.
- Santoro, A.E., Buchwald, C., McIlvin, M.R., Casciotti, K.L., 2011. Isotopic signature of N<sub>2</sub>O produced by marine ammonia-oxidizing archaea. *Science* 333, 1282–1285.
- Schloss, P.D., Westcott, S.L., Ryabin, T., Hall, J.R., Hartmann, M., Hollister, E.B., Lesniewski, R.A., Oakley, B.B., Parks, D.H., Robinson, C.J., Sahl, J.W., Stres, B., Thallinger, G.G., Van Horn, D.J., Weber, C.F., 2009. Introducing mothur: open-source, platform-independent, community-supported software for describing and comparing microbial communities. *Appl. Environ. Microbiol.* 75, 7537–7541.
- Shan, J., Zhao, X., Sheng, R., Xia, Y., Ti, C., Quan, X., Wang, S., Wei, W., Yan, X., 2016. Dissimilatory nitrate reduction processes in typical Chinese paddy soils: rates, relative contributions, and influencing factors. *Environ. Sci. Technol.* 50, 9972–9980.
- Smith, K.A., 1980. A model of the extent of anaerobic zones in aggregated soils, and its potential application to estimates of denitrification. *J. Soil Sci.* 31, 263–277.
- Song, G.D., Liu, S.M., Marchant, H., Kuypers, M.M.M., Lavik, G., 2013. Anaerobic ammonium oxidation, denitrification and dissimilatory nitrate reduction to ammonium in the East China Sea sediment. *Biogeochem. Discuss.* 10, 4671–4710.
- Sorensen, J., Tiedje, J.M., Firestone, R.B., 1980. Inhibition by sulfide of nitric and nitrous oxide reduction by denitrifying *Pseudomonas fluorescens*. *Appl. Environ. Microbiol.* 39, 105–108.
- Straub, K.L., Benz, M., Schink, B., Widdel, F., 1996. Anaerobic, nitrate-dependent microbial oxidation of ferrous iron. *Appl. Environ. Microbiol.* 62, 1458–1460.
- Tariq, J., Ashraf, M., Jaffar, M., Afzal, M., 1996. Pollution status of the Indus River, Pakistan, through heavy metal and macronutrient contents of fish, sediment and water. *Water Res.* 30, 1337–1344.
- Thamdrup, B., Dalsgaard, T., 2002. Production of N<sub>2</sub> through anaerobic ammonium oxidation coupled to nitrate reduction in marine sediments. *Appl. Environ. Microbiol.* 68, 1312–1318.
- Throbäck, I.N., Enwall, K., Jarvis, Å., Hallin, S., 2004. Reassessing PCR primers targeting nirS, nirK and nosZ genes for community surveys of denitrifying bacteria with DGGE. *FEMS Microbiol. Ecol.* 49, 401–417.
- Trimmer, M., Nicholls, J.C., Deflandre, B., 2003. Anaerobic ammonium oxidation measured in sediments along the Thames Estuary, United Kingdom. *Appl. Environ. Microbiol.* 69, 6447–6454.
- Vitousek, P.M., Howarth, R.W., 1991. Nitrogen limitation on land and in the sea: how can it occur? *Biogeochemistry* 13, 87–115.
- Wang, L., Zheng, B., Nan, B., Hu, P., 2014. Diversity of bacterial community and detection of nirS- and nirK-encoding denitrifying bacteria in sandy intertidal sediments along Laizhou Bay of Bohai Sea, China. *Mar. Pollut. Bull.* 88, 215–223.
- Wang, J., Du, J., Baskaran, M., Zhang, J., 2016. Mobile mud dynamics in the East China Sea elucidated using <sup>210</sup>Pb, <sup>137</sup>Cs, <sup>90</sup>Sr, and <sup>234</sup>Th as tracers. *Journal of Geophysical Research: Oceans* 121, 224–239.
- Wang, M., Tang, T., Burek, P., Havlík, P., Krisztin, T., Kroeze, C., Leclère, D., Stokal, M., Wada, Y., Wang, Y., Langan, S., 2019. Increasing nitrogen export to sea: a scenario analysis for the Indus River. *Sci. Total Environ.* 694, 133629.
- Ward, B.B., Devol, A.H., Rich, J.J., Chang, B.X., Bulow, S.E., Naik, H., Pratihary, A., Jayakumar, A., 2009. Denitrification as the dominant nitrogen loss process in the Arabian Sea. *Nature* 461, 78–81.
- Watanabe, T., Kojima, H., Umezawa, K., Hori, C., Takasuka, T.E., Kato, Y., Fukui, M., 2019. Genomes of neutrophilic sulfur-oxidizing chemolithoautotrophs representing 9 proteobacterial species from 8 genera. *Front. Microbiol.* 10, 316.
- Weber, K.A., Pollock, J., Cole, K.A., Susan, M., Connor, O., Achenbach, L.A., Coates, J.D., Betaproteobacterium, L., Connor, S.M.O., 2006. Anaerobic nitrate-dependent iron(II) bio-oxidation by a novel lithoautotrophic anaerobic nitrate-dependent iron(II) bio-oxidation by a novel. *Society* 72, 686–694.
- Yang, F., Wu, J., Zhang, D., Chen, Q., Zhang, Q., Cheng, X., 2018. Soil bacterial community composition and diversity in relation to edaphic properties and plant traits in grasslands of southern China. *Appl. Soil Ecol.* 128, 43–53.
- Yao, X.F., Zhang, J.M., Tian, L., Guo, J.H., 2017. The effect of heavy metal contamination on the bacterial community structure at Jiaozhou Bay, China. *Braz. J. Microbiol.* 48, 71–78.
- Yoshida, M., Ishii, S., Otsuka, S., Senoo, K., 2009. Temporal shifts in diversity and quantity of nirS and nirK in a rice paddy field soil. *Soil Biol. Biochem.* 41, 2044–2051.
- Yu, Z., Deng, H., Wang, D., Ye, M., Tan, Y., Li, Y., Chen, Z., Xu, S., 2013. Nitrous oxide emissions in the Shanghai river network: implications for the effects of urban sewage and IPCC methodology. *Glob. Chang. Biol.* 19, 2999–3010.
- Zhang, W.L., Zeng, C.S., Tong, C., Zhai, S.J., Lin, X., Gao, D.Z., 2015. Spatial distribution of phosphorus speciation in marsh sediments along a hydrologic gradient in a subtropical estuarine wetland, China. *Estuar. Coast. Shelf Sci.* 154, 30–38.

- Zheng, Y., Hou, L., Liu, M., Gao, J., Yin, G., Li, X., Deng, F., Lin, X., Jiang, X., Chen, F., Zong, H., Zhou, J., 2015. Diversity, abundance, and distribution of nirS-harboring denitrifiers in intertidal sediments of the Yangtze Estuary. *Microb. Ecol.* 70, 30–40.
- Zheng, Y., Hou, L., Liu, M., Yin, G., Gao, J., Jiang, X., Lin, X., Li, X., Yu, C., Wang, R., 2016. Community composition and activity of anaerobic ammonium oxidation bacteria in the rhizosphere of salt-marsh grass *Spartina alterniflora*. *Appl. Microbiol. Biotechnol.* 100, 8203–8212.
- Zheng, Y., Hou, L., Chen, F., Zhou, J., Liu, M., Yin, G., Gao, J., Han, P., 2019. Denitrifying anaerobic methane oxidation in intertidal marsh soils: occurrence and environmental significance. *Geoderma* 357, 113943.
- Zumft, W.G., 1997. Cell biology and molecular basis of denitrification. *Microbiology and Molecular Biology Reviews: MMBR* 61, 533–616.